



Rapid assessment of pork freshness using miniaturized NIR spectroscopy

Christopher T. Kucha¹ · Michael O. Ngadi¹

Received: 3 April 2019 / Accepted: 23 December 2019 / Published online: 3 January 2020
© Springer Science+Business Media, LLC, part of Springer Nature 2020

Abstract

The freshness of meat is an important quality attribute. Thiobarbituric Acid Reactive Substances (TBARS), a classical marker of lipid oxidation, is used as an indicator of freshness in meat. This study investigated the application of a miniaturized and portable Near Infrared (NIR) spectroscopy (1100–2200 nm) for rapid monitoring of TBARS in minced pork stored at 4 °C for 0, 2, 4 and 8 days. NIR data was pre-treated with standard normal variate (SNV), multiplicative scatter correction (MSC), and Savitzky Golay first derivative (FD). Models developed, based on full wavelengths, using partial least square regression (PLSR) showed good results in terms of their coefficients of determination (R^2). The optimized result was obtained from MSC with R^2 of 0.844 and RMSE of 0.099 mg MDA/kg meat in the prediction. To build a simpler model, optimal wavelengths were selected by successive projection algorithm (SPA) and weighted regression coefficients (RC) and used to develop four new models based on PLSR and MLR algorithms (SPA-PLSR, SPA-MLR, RC-PLSR, RC-MLR). The simplified model (RC-PLSR) revealed good results with R^2_p of 0.830 and RMSE of 0.068 mg MDA /kg meat. The promising result in this study indicated the potential of using a miniaturized NIR spectroscopy as a good handheld tool for rapid monitoring of TBARS values for assessment of freshness in minced pork.

Keywords Miniaturized NIR spectroscopy · Minced pork · TBARS · Partial least square regression

Introduction

The inspection and control of food has taken a new dimension. The development of fast, portable, easy and cheap analytical techniques for laboratory or regulatory control remains a focal point of research in the meat industry in recent times [1]. Near Infrared Spectroscopy (NIRS) technique possesses the above-mentioned requirements and have been used for evaluation of various freshness indicators in pork meat [2–6]. However, the current trend in spectroscopic techniques has shifted towards the construction of miniature and portable devices. This innovation is probably because the large and expensive benchtop devices may not be amenable for online application during processing or application along the value chain at the retail point of sale. Portable NIRS devices have been applied in the measurement

of meat quality attributes [7–10]. For example, Schmutzler, Beganovic, Böhler and Huck [7] used a portable NIR system for the non-destructive quality and safety measurement of veal sausages and reported improved accuracy when compared to large and high-performance spectrometers. These studies have demonstrated scientific evidence of using portable NIRS for quality assessment of meat and meat products.

Pork is a widely consumed meat, and Minced Pork (MP) is one of its products made from lean, trims, and other fatty portions of the carcass, and sold to the consumer with various levels of fat content. However, the process of grinding distorts the muscle membrane system and exposes the labile lipids components to oxygen in the air. The exposure causes lipid oxidation and eventually results in a loss of freshness and hence a decrease in the shelf-life [11]. Lipid oxidation produces primary products (hydroperoxide) that further decomposes to yield various low-molecular-weight secondary compounds including aldehydes, ketones, and alcohols [12]. These compounds are responsible for the off-flavor, off-odors and color changes that can be perceivable by consumers [13, 14]. Furthermore, they have biological effects on human health [15]. Therefore, lipid oxidation is a critical

✉ Michael O. Ngadi
michael.ngadi@mcgill.ca

¹ Department of Bioresource Engineering, McGill University, Macdonald Campus, 21,111 Lakeshore Road, Ste-Anne-de-Bellevue, QC H9X 3V9, Canada

factor that has a significant influence on the loss of freshness leading to both commercial and health consequences. Accordingly, strategies to develop and optimize measurement tools for monitoring meat freshness is necessary to ensure a safe and quality product to the consumer.

Several methods for monitoring lipid oxidation in meat based on primary and secondary changes have been reported [16]. Primary changes involve measurement of the hydroperoxide while secondary changes are based on the evaluation of the decomposed products of hydroperoxide [17]. Although various low-molecular-weight compounds are produced during the decomposition of hydroperoxide, malondialdehyde (MDA) is the most important and abundant aldehyde that is used as an oxidation index. Thiobarbituric acid reactive substances (TBARS) tests are commonly used to determine the extent of the formation of MDA in foods [18]. TBARS is a spectrophotometric method based on the stoichiometric reaction of MDA with Thiobarbituric acid (TBA) to yield a pinkish MDA-TBA complex [19]. While these methods are sensitive and straightforward, they are highly empirical, labor-intensive, and time-consuming. These drawbacks limit their application for rapid monitoring of TBARS level in meat.

Based on the MDA-TBA stoichiometric reactions, research has demonstrated that it is possible to evaluate TBARS of muscle foods using some optical methods, such as hyperspectral imaging [20–23]. One of the essential features of this technology is that it is capable of showing TBARS distribution in meat [24]. However, at present, hyperspectral imaging is expensive, and a large amount of data generated from the NIR images poses computation difficulties. Investigations employing spectroscopy in the visible range (360–740 nm) [25, 26] revealed that TBARS could be predicted with good results. For instance, Cifuni, Amici, Contò, Viola and Failla [25] investigated the use of spectroscopy for the rapid assessment of TBARS from the meat of wild boar, and Cifuni, Contò and Failla [26] explored the feasibility of monitoring TBARS in rabbit meat. Both studies yielded R^2_p of 0.843 and 0.834, respectively. In fish, Karlsdottir, Arason, Kristinsson and Sveinsdottir [27] found an R^2 of 0.80 in the validation set for fish using a Vis/NIR spectroscopy (400–2500 nm). One study [28] for pork using NIR spectroscopy (950–1650 nm) reported an R^2 of 0.657 using principal component regression. These studies were based on benchtop spectrometers.

Portable NIRS has the benefit of rapid monitoring of TBARS, a classical indicator of meat freshness, in minced pork. The possibility to assess freshness by a portable and handheld instrument could be a valuable tool at control points in the production and distribution chain without lengthy procedures of chemical methods. However, no studies have been reported on the use of a miniaturized and portable micro NIR spectrometer to assess TBARS even though

some published work have demonstrated their potential for non-destructive and rapid application in food [29]. Therefore, the objectives of this study were: (1) To investigate the reliability of a portable micro NIR spectrometer in the spectral region of 1100–2200 nm for predicting TBARS value of minced pork during low-temperature storage at 4 ± 1 °C for different lengths of time; and (2) To identify the optimal wavelengths and develop a simplified model for rapid predicting TBARS in minced pork. Minced meat was specifically chosen since it is especially vulnerable to oxidation.

Materials and methods

Sample preparation

Minced pork samples were bought from a grocery store in Montreal, Canada. The minced meat was made from fresh meat after a 24-h aging period. The meat was made after the addition of about 20% backfat. The samples were wrapped in vacuum packs and transported to the Food and Bioprocess Engineering laboratory of McGill University. The shipping was carried out at 4 °C. The samples were distributed in plastic lidded Petri-dishes. A total of 80 subsamples were prepared and randomly assigned to four groups of 20. After the fresh subsamples (day 0) were immediately scanned, the remaining three groups were stored at 4 °C for 2, 4 and 8 days. At the end of each storage period, the subsamples were scanned and the TBARS reference values determined. To avoid bias in the selection of calibration and prediction sets during the model development, the classic Kennard–Stone (KS) algorithm was applied. The implementation of this method has been described by Casale, Casolino, Oliveri and Forina [30].

Determination of reference values of TBARS

TBARS values were determined in triplicate for the total number of samples ($n = 80$) by a modified extraction method of [20]. For the extraction, 5 g of minced pork was homogenized with 20 ml of 20% trichloro acetic acid (TCA) and 20 ml of double distilled water. The mixture was kept for 1 h. It was then centrifuged for 10 min at a speed of 2000 rpm. The supernatant was filtered through a number 1 Whatman filter paper. A 5 ml of the filtrate was added to a 5 ml of 0.02 M solution of TBA. The mixture was heated at 95 °C for 20 min and then removed and cooled under running tap water. The absorbance was immediately measured at 532 nm against a blank containing one ml distilled water and one ml TCA and 2 ml TBA reagent using a UV spectrophotometer (Unicam-UV1, Thermos spectronic Inc., NY). Results expressed as mg MDA/kg meat were calculated from the standard curve of 1,1,3,3-tetramethoxypropane.

NIR spectrometer system

In this study, the JDSU MicroNIR 2200 spectrometer (E1-00184 version 1.5.7) was used. The system has a spectral range of 1100–2200 nm and a bandwidth of 8.15 nm and wavelengths of 125 nm. It is of a palm size with a weight of 60 g and 50 mm in diameter. Its components such as the light source, optics dispersing elements, a linear detector array, are all contained within the unit making it possible to be easily carried around. The spectrometer can be powered by a USB from a laptop or a tablet. The portability of the instrument would make it convenient for monitoring lipid degradation in pork at the processing plant, at a grocery store during refrigerated display. It could even be simply carried by a meat regulatory or an enforcement agent. The technology is based on the high-reliability linear variable filter (LVF). The principle of operation of the JDSU MicroNIR spectrometer has been discussed elsewhere [31].

NIRS measurement

The minced pork was scanned, and the data were collected in the reflectance mode by using the JDSU MicroNIR spectrometer, which was connected to a desktop computer through a USB cable. Calibration of the instrument was carried out using the black (~0% reflectance) opaque cap to completely cover the sapphire window and acquired the dark reference spectrum. Following the dark calibration, the white diffuse reference standard (~99% reflectance) was also used to collect the spectrum of the standard. The white and dark reference spectra were collected to correct the environmental and the instrumental influences on the collected spectrum of the samples. For the acquisition of the spectra, the sapphire window of the MicroNIR spectrometer was placed directly in contact with the Petri-dish containing the minced pork. To avoid possible effects due to differences in the minced meat composition, each spectrum was the average of measurement of three spectra on the same Petri-dish. The spectra were collected with an integration time of 5600 μ s at around 22 ± 2 °C in the laboratory.

Multivariate analysis

Spectral pre-processing

The calibration equations were developed from a partial least square regression (PLSR) using the cross-validation method. PLSR is a widely used regression modeling method which finds a satisfactory solution in cases where a linear relationship exists between the spectra and the target analyte. It has shown robustness in the development of a calibration model for TBARS evaluation using spectral techniques [22, 24]. These studies demonstrates that there is a linear relationship

between NIR spectral data and TBARS in meat. To optimize the calibration models, NIR data was first pre-treated. It was necessary to perform pre-treatments since NIR spectra are easily affected by physical properties of the analyzed products and other interferences. For the minced pork in this study, the variations in average particle size, distribution of particle shapes, the density of packing and the presence of voids in the minced pork will lead to the unwanted baseline fluctuations in NIR reflectance spectra which may result to complex intensity variations. Thus, mathematical pre-treatments removes unwanted noise and improves the signal to noise ratio. In this study, standard normal variate (SNV), multiplicative scatter correction (MSC), and Savitzky Golay first derivative (FD), were applied to pre-treat the spectra data. SNV is a mathematical transformation method used to remove slope variation and to correct for scattering. Each spectrum is corrected by centering the spectral values, scaling the centered spectrum by the standard deviation calculated from individual spectral values. On the other hand, MSC reduces the effects of scattering on spectra data by using least squares to fit individual spectrum to the average spectrum [32]. FD is equally powerful in correcting baseline shifts by estimating the difference between two subsequent spectra [33]. All the spectral preprocessing procedures were executed in the PLS Toolbox running under Matlab 2018b (The Mathworks Inc., Natick, MA, USA).

Model calibration based on full wavelengths

The samples were divided into calibration ($n = 56$, range 0.020–0.813 mg MDA/kg minced meat) and prediction ($n = 24$, range = 0.018–0.789 mg MDA/kg minced meat) sets using the Kernard-Stone approach mentioned above. The calibration samples were used to make a regression model which could be applied as a reference against spectral from independent prediction samples. This calibration was necessary to illustrate the possibility of NIR spectrometer for TBARS measurement for future predictions. In this study, multivariate linear algorithms of partial least squares regression (PLSR), was used to develop models from the spectral data and the reference TBARS values. PLSR is a powerful chemometric method that is particularly suitable where the number of variables is more than the number of samples. In PLSR, the latent variables which represent most of the information in the spectral data are correlated with the reference values according to the lowest values of the prediction residual error sum of squares (PRESS) [34]. The PLSR models were built with the calibration set under the approach of cross-validation by the venetian blind method [35]. The models were built using the PLS Toolbox running under Matlab 2018b (The Mathworks Inc., Natick, MA, USA) environment. SIMPLS was used as the PLS engine function.

Model calibration based on optimal wavelengths

The NIR spectra contain multiple sets of variables (wavelengths) with overlapping information. That is, the acquired spectra data from the minced pork samples were composed of redundant multi-collinearity (or spectra correlated) information among contiguous wavelengths, which were not relevant to predicting TBARS. The selection of characteristic wavelengths is an important task because of the simpler models as well as the non-informative wavelengths that are discarded [36]. The removal of the redundant information by multivariate data analysis makes it possible to extract useful information from original data, eliminate much overlapping information, and reduce the dimension of data. Also, simpler models could be used for the purpose of developing multispectral spectrometer systems for real-time application. In this study, the weighted regression coefficients (RC) and successive projection algorithm (SPA) were used to select the optimal wavelengths. RC is a powerful wavelength selection method. In this technique, the spectral data is first standardized by dividing each spectrum by its standard deviation to ensure that each variable had the same variance. The PLSR model is then developed between the standardized spectral data and the reference analyte values, which yields the RC. Since all variables are adjusted to the same scale, the resulting coefficients show the relative importance of the wavelengths in the model. Wavelengths having large absolute RC from the PLSR cross-validation model are considered as important feature wavelengths [34]. On the other hand, SPA is a variable selection algorithm designed to select wavelengths with minimal redundant information. The method employs a simple projection operation in a vector space to select subsets of variables with a minimum of collinearity. The variable selected by SPA has the maximum projection value on the orthogonal subspace of the previous selected variable. SPA involves three main steps. The first step consists of projections on the columns of the spectral matrix, which generate candidate subsets of variables with minimum collinearity. The second step involves evaluating candidate subsets of variables based on the value of root mean square error (RMSE) obtained from validation set of MLR calibration. The final step is removing variables that contribute to high RMSE through an elimination procedure without significant loss of prediction capability [22]. The selected wavelengths were used to build new calibration models using PLSR and multilinear regression (MLR). MLR is a regression

method that is applicable where the number of variables is less than the number of samples [37]. The selection of optimal wavelengths by SPA was performed in Matlab R2018b (The Mathworks Inc., Natick, MA, USA).

Model validation and evaluation

The calibration models developed from PLSR and MLR were validated by using an independent prediction set samples. For each of the models, the predictive abilities were evaluated by four statistics criteria, i.e., the coefficients of determination (R^2), root mean square of calibration ($RMSE_c$), root mean square error of cross-validation ($RMSE_{cv}$), and root means square error of prediction ($RMSE_p$). The R^2 denoted the percentage of the variation in the response variables (TBARS values) that were explained by the spectral data matrix. The $RMSE_c$, $RMSE_{cv}$, and $RMSE_p$ indicated the degree of fitting of the regression during the calibration, cross-validation and prediction procedures. Good models are usually appraised by low $RMSE_c$, $RMSE_{cv}$ and, $RMSE_p$, high R^2_c , R^2_{cv} , and R^2_p as well as small differences between $RMSE_c$, $RMSE_{cv}$, and $RMSE_p$.

Results and discussion

Statistics of TBARS of all tested samples

The mean, range and standard deviation of the TBARS concentration observed in each storage case are presented in Table 1. There were some considerable differences in the concentration of TBARS as the storage time increased, ranging from 0.020 to 0.911 mg MDA/kg meat. The TBARS showed lower values from day 0 to day 8 and at 12 days of storage, the values were relatively higher. These results are similar to those reported by Ramírez and Cava [38], Orkusz,

Table 1 Statistics TBARS of minced pork samples (mg MDA/kg minced pork)

Storage time (days)	Mean	Max	Min	Std
0	0.103	0.201	0.020	0.058
2	0.362	0.557	0.262	0.051
4	0.377	0.453	0.265	0.072
8	0.709	0.911	0.452	0.245

Haraf, Okruszek and Werekńska-Sudnik [39], Wu, Song, Qiu and He [24], Cifuni, Contò and Failla [26].

Analysis of spectral characteristics and preprocessing

The NIR spectra indicated noticeable the reflectance differences at different lengths of storage time (0, 2, 4, and 8 days) at 4 °C with quite a similar shapes and characteristic peaks and valleys throughout the NIR range (1100–2200 nm) (Fig. 1). Thus, important features of reflectance bands of C–H stretching second overtone at 1207 nm corresponded to fat [40–42]; O–H stretching first overtone at 1450 nm could be related to water [43]; N–H stretching at 1500 nm could be related to protein [40, 44]; C–H combination overtone at 2063 nm may also be related to fat [45]. Also, there was an increase in reflectance intensity as the storage time increased, suggesting that there was variation in chemical composition as aging proceeds. The spectrum at day 0 showed the lowest reflectance values relative to the other storage periods (2, 4, and 8 days). The increase in reflectance values could be attributed to the decrease in pH as aging progressed which increased the protein denaturation and precipitation of the sarcoplasmic protein over the storage time [22]. Furthermore, besides protein denaturation caused by low pH, decomposition reactions are reported to accumulate lipid oxidation products [20], which could cause a structural and functional change in proteins [46], that might could also contribute to the low reflectance intensity observed over the storage time in this study. It is evident from the spectra that

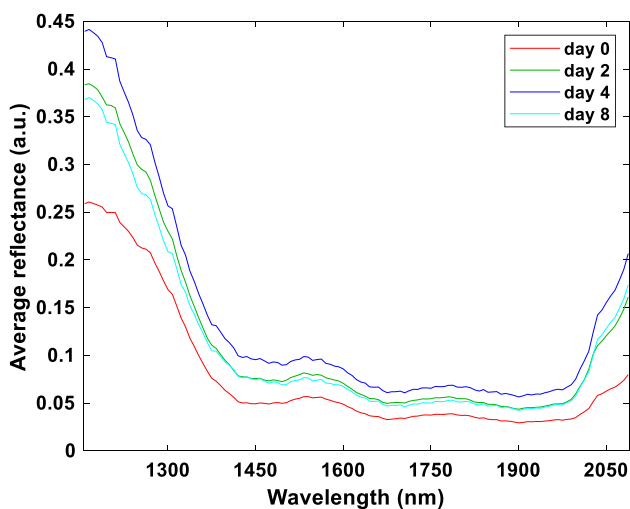


Fig. 1 Average spectral profiles of the minced pork during cold storage at 4 °C

the reflectance values at day 12 exhibited somewhat different behavior from the other storage periods across the entire wavelength region examined. It was expected that day 12 would have the highest reflectance values in the going trend. Contrary, the spectra were located between day 0 and day 4 with some overlap at higher wavelengths. The lower reflectance intensity noticed at day 8 may be as a result of the decrease in TBARS value induced by the decomposition of aldehydes (i.e. oxidative products) which interacted with the muscle proteins [22]. This observation was also reported by Cheng, Sun, Pu, Wang and Chen [20] in their study to develop a rapid method based on hyperspectral imaging for evaluation of TBARS in stored grass carp fillets.

Scatter correction methods and spectral derivatives are the two most frequently used categories of pre-processing techniques. The purpose of scatter correction methods is to reduce the scatter effects which occur between samples. Whereas derivatives can remove baseline effects and any offset differences between the data. As previously noted, the average particle size and density of packing create voids within the minced meat which apparently created light scattering effect that eventually introduce a baseline shift in the spectra profiles. However, by application of suitable pre-processing methods, these effects were largely eliminated. Since scatter effects are inevitable in spectroscopic methods, the spectra were corrected by the application of different mathematical treatments, namely, SNV, MSC, FD. The resulting transformed spectral profiles for the stored minced pork are presented in Fig. 2. It is evident that all the spectra treatments affected the spectral profile. The differences in the resulting spectral profile reveal the impact of the preprocessing methods. Whereas SNV and MSC tended to maintain the same spectral pattern, MSC maintained a similar scale as the original NP.

Spectral variation among tested samples

Before the development of the calibration model, principal component analysis (PCA) was performed on the NIR data to visualize the primary sources of variation in the data. PCA is generally used as a mathematical method for the classification of samples. In this study, the first two principal components explained 95.04% of the total sample variation, as illustrated in the PCA score plot (Fig. 3). All the samples were clustered into four groups based on the storage time. There was some overlap among the samples, especially day eight samples, which could be as a result of the differences in the level of degradation. It was also visually observed that as aging time increased, the color change became more pronounced primarily due to oxidation processes.

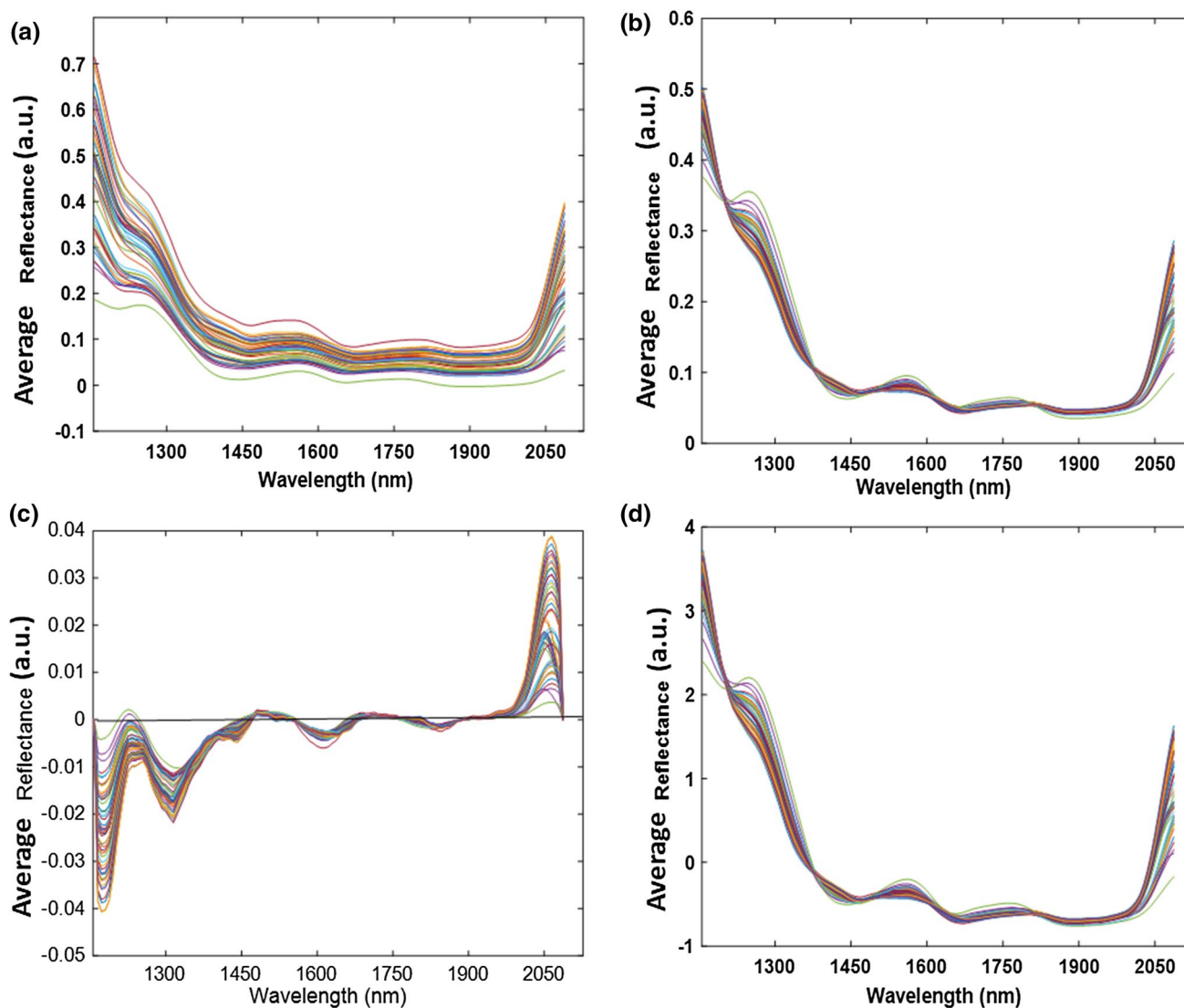


Fig. 2 Preprocessed spectra of the minced pork. **a** NP; **b** MSC; **c** FD; and **d** SNV

Prediction of TBARS value based on full wavelengths

Table 2 shows the performances of the developed models for assessment of TBARS value in minced pork in the calibration, cross-validation, and prediction. The models were developed using raw and pre-processed spectra of the samples at full wavelengths (1100–2200 nm) and the reference values of TBARS. The results revealed that the model

developed from the non-processed (NP) data (i.e. the raw data) yielded a good result ($R^2_p=0.780$, $RMSEP=0.080$ mg MDA/kg). Three additional models (SNV-PLSR, MSC-PLSR, and FD-PLSR) were provided from the spectral data pre-treated with SNV, MSC, and FD.

The results presented in Table 2 show that regression models based on different preprocessing techniques (MSC, FD, SNV) produced higher R^2_p and lower $RMSEP$ in comparison to the models based on the unprocessed spectra

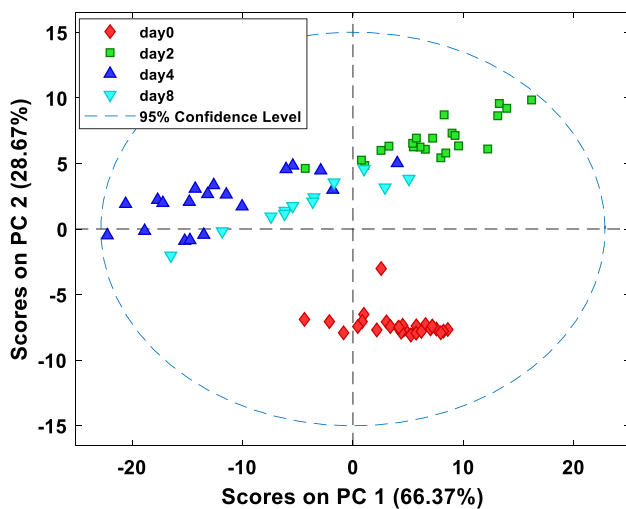


Fig. 3 Classification of minced pork meat by principal component analysis as a function of storage time (0, 4, 8, and 12 days at 4 °C)

(NP). The undesirable impact of the scatter effects on the regression models was proven by the poor predictive ability obtained when the PLSR model was developed from the original data to determine the TBARS value. Among the pre-processing methods applied, FD pre-processed spectra dataset provided the poorest model results ($R^2_p = 0.748$, $RMSEP = 0.069$). This was probably because part of the information removed from the spectra data by applying this technique may be useful for measuring the TBARS value in the minced pork. On the other hand, with the SNV pre-processed spectra, a modest improvement of the predictive ability of the PLS model ($R^2_p = 0.810$, $RMSEP = 0.067$) was obtained with a unit decrease in the PLS latent variables.

This finding demonstrated that SNV is a useful tool for improving the PLSR model for predicting TBARS in the minced samples by correcting scatter effects. Much better PLSR model was found when the spectral data was pre-processed with MSC (R^2_p and $RMSEP$ of 0.844 and 0.088). Therefore, MSC was selected as the optimal pre-processing method which was in agreement with other reports [20, 22]. The superiority of MSC pre-processing treatment over FD and SNV pre-processing methods could be that it was more powerful in sufficiently removing the unwanted effects by the light scattering induced by the inhomogeneous morphology in the minced pork. Moreover, as could be seen in the spectral plots represented in Fig. 2, where similar patterns were found between MSC and SNV spectra datasets, the performance of models based on these two spectral pre-processing methods gave higher PLSR model results compared to the FD pre-processed dataset.

Prediction of TBARS value based on optimal wavelengths

Selecting informative wavelengths from spectral regions that would accurately describe an analyte do not improve model performance at all times. In certain cases, it may actually degrade model performance. This typically happens when selected or chosen variables do not contribute positively to the model or when important variables are removed. Generally, the wavelengths with little influence on the prediction model are useless and are removed from the specific application so that a simpler model could be developed with the potential of developing a multispectral system based on those specific wavelengths. Considering that MSC pre-treated data yielded the best model, the optimal wavelengths

Table 2 Regression models for predicting TBARS values in minced pork meat

Model	Variable #	Latent Var	Calibration		Cross-validation		Prediction	
			R^2_c	$RMSE_c$	R^2_{cv}	$RMSE_{cv}$	R^2_p	$RMSEP_p$
NP-PLSR	125	7	0.821	0.073	0.806	0.065	0.780	0.080
SNV-PLSR	125	6	0.802	0.070	0.791	0.074	0.810	0.067
MSC-PLSR	125	7	0.887	0.075	0.876	0.079	0.844	0.088
FD-PLSR	125	7	0.839	0.067	0.821	0.071	0.748	0.069
SPA-PLSR	15	9	0.870	0.061	0.851	0.065	0.820	0.059
SPA-MLR	15	/	0.819	0.081	0.798	0.087	0.782	0.092
RC-PLSR	15	8	0.883	0.056	0.852	0.063	0.830	0.068
RC-MLR	15	/	0.835	0.078	0.824	0.084	0.787	0.087

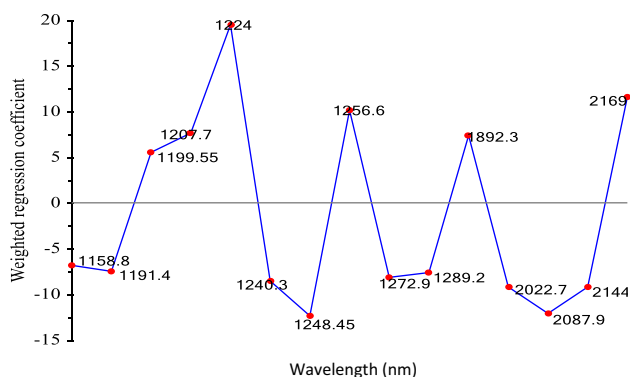


Fig. 4 The selection of optimal wavelengths by weighted regression coefficients

were selected from the MSC transformed data by SPA and RC. RC provided fifteen wavelengths (1159, 2169, 1680, 1640, 1257, 1583, 1371, 1485, 1876, 1183, 1306, 1208, 1347, 2121, 2145 nm) (Fig. 4), and fifteen optimal wavelengths (1159, 1191, 1200, 1208, 1224, 1240, 1250, 1257, 1273, 1289, 1892, 2023, 2088, 2145, 2169 nm) were identified by SPA (Fig. 5).

It was observed that SPA selected wavelengths that cut across the entire NIR range. These wavelengths can be attributed to some compositional information because chemical bonds ($-\text{CH}_2$, $-\text{CH}_3$, and $-\text{CH}=\text{CH}-$) absorb light energy at specific wavelengths. According to [47], the wavelengths located at 1100–1300, 1300–1600, 1600–1850, 1850–2050, and 2050–2230 nm are characteristics of C–H second overtone, C–H first overtone and combination bands, C–H first overtone, C–H and O–H combination bands, and C–H combination band, respectively. Therefore, at 1100–1300 nm region, SPA selected nine wavelengths (1159, 1191, 1200, 1208, 1224, 1240, 1250, 1257, 1273, 1289 nm) which showed remarkable bands related to fat and represented 60% of the total wavelengths for building the calibration models. The wavelengths at 1159, 1191, 1200, and 1208, 1224 nm could be associated with fat since wavelengths closed to 1200 nm, which are a fundamental constituent of fatty acid molecules absorb strongly [48]. Moreover, the wavelength at 1892, associated with C–H first overtone corresponding could be associated with fat. For the N–H combination bands, 2023, 2088, 2145, and 2169 nm were selected, which could be due to protein [49]. The generation of such

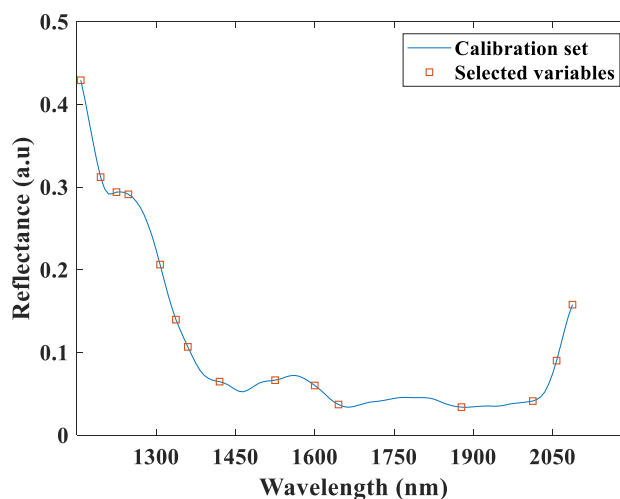


Fig. 5 The selection of optimal wavelengths by SPA

a contribution from fat and protein bands may mean that there could be some correlation between protein and fat in the samples during aging.

By this selection, four new models based on PLSR and MLR algorithms (SPA-PLSR, SPA-MLR, RC-PLSR, RC-MLR) were built (Table 2). However, in some cases, the new models based on these reduced wavelengths were slightly lower in predictive capabilities than the MSC-PLSR model (Table 2). Nevertheless, the new models could be used to develop a multispectral spectrometer for monitoring TBARS value in minced pork. RC-PLSR showed a closely prediction capability ($R^2_p = 0.830$, $\text{RMSE}_p = 0.068$ mg MDA/kg) to the MSC-PLSR. The optimal wavelengths from RC were used to obtain predictive regression equations for TBARS value in the NIR range (1100–2200 nm) as follows:

$$\begin{aligned}
 Y_{\text{TBARS}} = & 4.3783 - 6.803 \times X_{1158.8\text{nm}} - 7.515 \times X_{1191.4\text{nm}} \\
 & + 5.555 \times X_{1199.55\text{nm}} + 7.6836 \times X_{1207.7\text{nm}} \\
 & + 19.431 \times X_{1224\text{nm}} - 8.500 \times X_{1240.3\text{nm}} \\
 & - 12.428 \times X_{1248.45\text{nm}} + 10.168 \times X_{1256.6\text{nm}} \\
 & - 8.127 \times X_{1272.9\text{nm}} - 7.633 \times X_{1289.2\text{nm}} \\
 & + 7.394 \times X_{1892.3\text{nm}} + 9.265 \times X_{2022.7\text{nm}} \\
 & - 12.078 \times X_{2087.9\text{nm}} - 9.247 \times X_{2144.95\text{nm}} \\
 & + 11.591 \times X_{2169.4\text{nm}}
 \end{aligned}$$

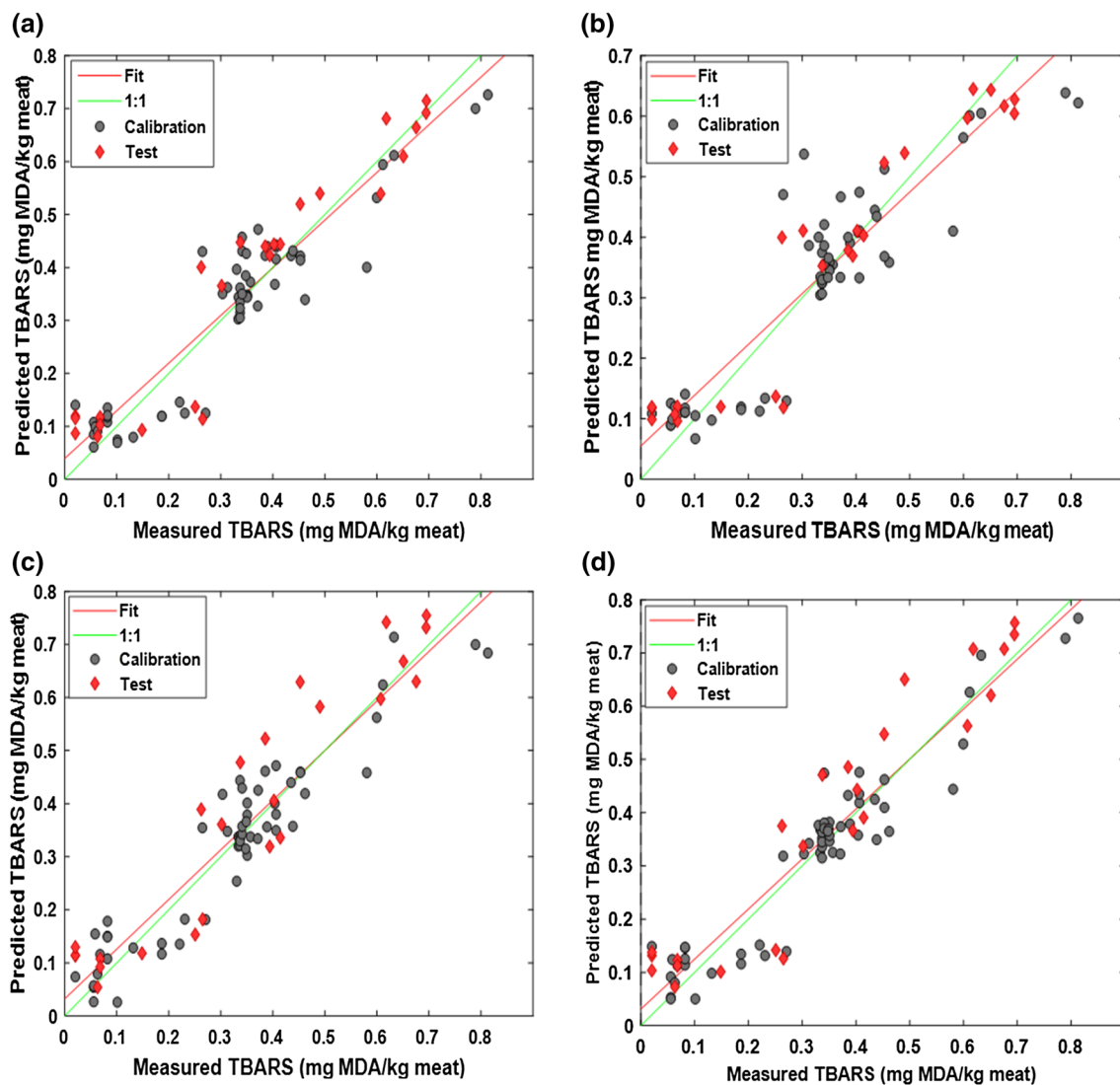


Fig. 6 Comparison of predicted and measured TBARS values by optimised models **a** NP=PLSR; **b** MSC-PLSR; **c** RC-PLSR; **d** SPA-PLSR 6

where X_i denotes the spectral reflectance value at the wavelength of i nm, Y_{TBARS} is the predicted TBARS value. The scatter plots of predicted versus measured values of the optimal wavelengths based on PLSR and MLR are presented in Fig. 6. It was shown that the meat samples were closely distributed to the regression lines in both models showing good performance of TBARS value prediction in minced pork using the ultra-compact miniaturized NIR spectroscopy. Fig. 6.

Conclusions

This study investigated the possibility of using a portable NIR spectroscopy for rapid and non-destructive monitoring of TBARS in minced pork. Pre-processing methods of SNV, MSC, first derivative, and second derivative were applied and compared. The PLSR models developed from the NIR pre-treated data revealed a good performance in coefficients of determination for the calibration, validation,

and prediction ($R^2_c \geq 0.802$, $R^2_{cv} \geq 0.791$, $R^2_p \geq 0.748$) for prediction of TBARS concentration. The MSC pretreated NIR spectra showed the optimal result ($R^2_c = 0.887$, $R^2_{cv} = 0.876$, $R^2_p = 0.844$). Based on the MSC-PLSR established model, fifteen optimal wavelengths (1158.8, 1191.4, 1199.55, 1207.7, 1224, 1240.3, 1248.45, 1256.6, 1272.9, 1289.2, 1892.3, 2022.7, 2087.9, 2144.95, 2169.4 nm) from the highest regression coefficients were selected and used to build new calibration models (PLSR and MLR). The results revealed that regression coefficient based on PLSR model ($R^2_p = 0.830$) outperformed that of MLR ($R^2_p = 0.787$). The promising result in this study shows the potential of using a miniaturized and portable MicroNIR. The instrument is a palm-size that is suitable as a handheld device. Chemometric incorporated with the spectrometer could be an excellent alternative to the time-consuming and expensive methods for monitoring TBARS for meat freshness assessment. The selected wavelengths would be used to develop a rapid multispectral spectrometer for an industrial application. More samples would be needed to validate the predictive accuracy for TBARS concentration monitoring in a future application.

References

- H.I. Kademi, B.H. Ulusoy and C. Hecker, *Food Rev. Int.* **35**, 201–220 (2019). <https://doi.org/10.1080/87559129.2018.1514624>
- S. Lee, T. G. Noh, J. H. Choi, J. Han, J. Y. Ha, J. Y. Lee, Y. Park, *Proc.SPIE*, (2017) <https://doi.org/10.1117/12.2261803>
- X. Wu, H. Fu, X. Tian, B. Wu, J. Sun, *J. Food Process Eng.* **40**, e12566 (2017). <https://doi.org/10.1111/jfpe.12566>
- X. Wang, M. Zhao, R. Ju, Q. Song, D. Hua, C. Wang, T. Chen, *Comput. Electron. Agric.* **99**, 41–53 (2013). <https://doi.org/10.1016/j.compag.2013.08.025>
- K. Horváth, Z. Seregély, É. Andrassy, I. Dalmadi, J. Farkas, *Acta Aliment.* **37**, 93–102 (2008). <https://doi.org/10.1556/AALim.37.2008.1.9>
- F. Qu, D. Ren, Y. He, P. Nie, L. Lin, C. Cai, T. Dong, *Meat Sci.* **146**, 59–67 (2018). <https://doi.org/10.1016/j.meatsci.2018.07.023>
- M. Schmutzler, A. Beganovic, G. Böhrer, C.W. Huck, *NIR News* **27**, 11–13 (2016). <https://doi.org/10.1255/nirn.1610>
- W. Wei, Y. Peng, L. Qiao, *Proc.SPIE*, (2016). <https://doi.org/10.1117/12.2223300>
- E. Zamora-Rojas, D. Marín, E. De Pedro-Sanz, J.E. Ginel, A. -Varo, *Meat Sci.* **90**, 636–642 (2012). <https://doi.org/10.1016/j.meatsci.2011.10.006>
- W. Wang, Y. Peng, F. Wang, H. Sun, *Proc. SPIE* **10217**, 102170R (2017). <https://doi.org/10.1117/12.2262508>
- M. Juárez, M.E.R. Dugan, L.L. Larsen, R. Thacker, D.C. Rolland, J.L. Aalhus, *Can J Anim Sci* **91**, 623–634 (2011). <https://doi.org/10.4141/cjas2011-059>
- E.N. Frankel, *J. Am. Oil Chem. Soc.* **61**, 1908–1917 (1984). <https://doi.org/10.1007/bf02540830>
- P.R. Sheard, M. Enser, J.D. Wood, G.R. Nute, B.P. Gill, R.I. Richardson, *Meat Sci.* **55**, 213–221 (2000). [https://doi.org/10.1016/S0309-1740\(99\)00145-X](https://doi.org/10.1016/S0309-1740(99)00145-X)
- B. Barriuso, I. Astiasarán, D. Ansorena, *Eur. Food Res. Technol.* **236**, 1–15 (2013). <https://doi.org/10.1007/s00217-012-1866-9>
- K.V. Ramana, S. Srivastava, S.S. Singhal, *Oxid. Med. Cell. Longev.* **2013**, 3 (2013). <https://doi.org/10.1155/2013/583438>
- J.I. Gray, F.J. Monahan, *Trends Food Sci. Technol.* **3**, 315–319 (1992). [https://doi.org/10.1016/S0924-2244\(10\)80019-6](https://doi.org/10.1016/S0924-2244(10)80019-6)
- C.T. Kucha, L. Liu and M.O. Ngadi, *Sensors (Basel, Switzerland)* **18**, 377 (2018). <https://doi.org/10.3390/s18020377>
- D.V. Hoyland, A.J. Taylor, *Food Chem.* **40**, 271–291 (1991). [https://doi.org/10.1016/0308-8146\(91\)90112-2](https://doi.org/10.1016/0308-8146(91)90112-2)
- J. Fernández, J.A. Álvarez, J.A. Fernández-López, *Food Chem.* **59**, 345–353 (1997). [https://doi.org/10.1016/S0308-8146\(96\)00114-8](https://doi.org/10.1016/S0308-8146(96)00114-8)
- J.-H. Cheng, D.-W. Sun, H.-B. Pu, Q.-J. Wang, Y.-N. Chen, *Food Chem.* **171**, 258–265 (2015). <https://doi.org/10.1016/j.foodchem.2014.08.124>
- J.-H. Cheng, D.-W. Sun, J.-H. Qu, H.-B. Pu, X.-C. Zhang, Z. Song, X. Chen, H. Zhang, *J. Food Eng.* **182**, 9–17 (2016). <https://doi.org/10.1016/j.jfoodeng.2016.02.004>
- Z. Xiong, D.-W. Sun, H. Pu, A. Xie, Z. Han, M. Luo, *Food Chem.* **179**, 175–181 (2015). <https://doi.org/10.1016/j.foodchem.2015.01.116>
- J.-L. Xu, C. Riccioli, D.-W. Sun, *J. Food Eng.* **169**, 259–271 (2016). <https://doi.org/10.1016/j.jfoodeng.2015.08.015>
- X. Wu, X. Song, Z. Qiu, Y. He, *Meat Sci.* **113**, 92–96 (2016). <https://doi.org/10.1016/j.meatsci.2015.11.008>
- G.F. Cifuni, A. Amici, M. Contò, P. Viola, S. Failla, *Eur. J. Wildl. Res.* **60**, 519–526 (2014). <https://doi.org/10.1007/s10344-014-0814-3>
- G.F. Cifuni, M. Contò, S. Failla, *J. Food Eng.* **169**, 85–90 (2016). <https://doi.org/10.1016/j.jfoodeng.2015.08.029>
- M.G. Karlsdottir, S. Arason, H.G. Kristinsson, K. Sveinsdottir, *Food Chem.* **159**, 420–427 (2014). <https://doi.org/10.1016/j.foodchem.2014.03.050>
- T.S. Park, Y.M. Bae, H.S. Seo, T.J. Park, K.H. Seol, D.K. Lim, M. Lee, S.I. Cho, *Biol. Eng.* **1**, 173–180 (2008). <https://doi.org/10.13031/2013.24477>
- E.J.N. Marques, S.T. de Freitas, M.F. Pimentel, C. Pasquini, *Food Chem.* **197**, 1207–1214 (2016). <https://doi.org/10.1016/j.foodchem.2015.11.080>
- M. Casale, C. Casolino, P. Oliveri, M. Forina, *Food Chem.* **118**, 163–170 (2010). <https://doi.org/10.1016/j.foodchem.2009.04.091>
- M. Alcalà, M. Blanco, D. Moyano, N. Broad, N. O'Brien, D. Friedrich, F. Pfeifer, H. Siesler, *J. Near Infrared Spectrosc.* **21**, 445–457 (2013)
- G.H. Geesink, F.H. Schreutelkamp, R. Frankhuizen, H.W. Vedder, N.M. Faber, R.W. Kranen, M.A. Gerritzen, *Meat Sci.* **65**, 661–668 (2003). [https://doi.org/10.1016/S0309-1740\(02\)00269-3](https://doi.org/10.1016/S0309-1740(02)00269-3)
- Q. Dai, D.-W. Sun, J.-H. Cheng, H. Pu, X.-A. Zeng and Z. Xiong, *Compr. Rev. Food Sci. Food Saf.*, **13**, 1207–1218 (2014). <https://doi.org/10.1111/1541-4337.12110>
- M. Kamruzzaman, Y. Makino, S. Oshita, *LWT Food Sci. Technol.* **66**, 685–691 (2016). <https://doi.org/10.1016/j.lwt.2015.11.021>
- D. Ballabio, V. Consonni, *Anal. Methods* **5**, 3790–3798 (2013). <https://doi.org/10.1039/C3AY40582F>
- D. Yang, D. He, A. Lu, D. Ren, J. Wang, *Infrared Phys. Technol.* **83**, 206–216 (2017). <https://doi.org/10.1016/j.infrared.2017.05.005>
- Q. Dai, D.-W. Sun, Z. Xiong, J.-H. Cheng, X.-A. Zeng, *Compr. Rev. Food Sci. Food Saf.* **13**, 891–905 (2014). <https://doi.org/10.1111/1541-4337.12088>
- R. Ramírez, R. Cava, *Meat Sci.* **75**, 388–396 (2007). <https://doi.org/10.1016/j.meatsci.2006.08.003>
- A. Orkus, G. Haraf, A. Okruszek, M. Werenńska-Sudnik, *Poult. Sci.* (2016). <https://doi.org/10.3382/ps/pew325>
- D.F. Barbin, G. ElMasry, D.-W. Sun, P. Allen, *Food Chem.* **138**, 1162–1171 (2013). <https://doi.org/10.1016/j.foodchem.2012.11.120>

41. N. Barlocco, A. Vadell, F. Ballesteros, G. Galietta, D. Cozzolino, *Anim. Sci.* **82**, 111–116 (2006). <https://doi.org/10.1079/ASC20055>
42. H. Huang, L. Liu, M.O. Ngadi, C. Gariépy, *Talanta* **119**, 385–395 (2014). <https://doi.org/10.1016/j.talanta.2013.11.015>
43. N. Prieto, R. Roehe, P. Lavín, G. Batten, S. Andrés, *Meat Sci.* **83**, 175–186 (2009). <https://doi.org/10.1016/j.meatsci.2009.04.016>
44. B. Park, Y.R. Chen, W.R. Hruschka, S.D. Shackelford, M. Koohmaraie, *Trans. Am. Soc. Agric. Eng.* **44**, 609 (2001). <https://doi.org/10.13031/2013.6087>
45. J. Brøndum, D.V. Byrne, L.S. Bak, G. Bertelsen, S.B. Engelsen, *Meat Sci.* **54**, 83–95 (2000). [https://doi.org/10.1016/S0309-1740\(99\)00085-6](https://doi.org/10.1016/S0309-1740(99)00085-6)
46. D.M. Smith, *J. Food Sci.* **52**, 22–27 (1987). <https://doi.org/10.1111/j.1365-2621.1987.tb13965.x>
47. P. Hourant, V. Baeten, M.T. Morales, M. Meurens, R. Aparicio, *Appl. Spectrosc.* **54**, 1168–1174 (2000)
48. V. Somovilla, F. España-España, A.J. Gaitán-Jurado, J. Aparicio, E.J. De Pedro-Sanz, *Food Chem.* **101**, 1031–1040 (2007). <https://doi.org/10.1016/j.foodchem.2006.02.058>
49. P. Ritthiruangdej, R. Ritthiron, H. Shinzawa, Y. Ozaki, *Food Chem.* **129**, 684–692 (2011). <https://doi.org/10.1016/j.foodchem.2011.04.110>

Publisher's Note Springer Nature remains neutral with regard to jurisdictional claims in published maps and institutional affiliations.